JOM, Vol. 70, No. 3, 2018
https://doi.org/10.1007/s11837-017-2668-0

SOLID FREEFORM FABRICATION

Effect of Bed Temperature on the Laser Energy Required to Sinter Copper Nanoparticles

N.K. ROY,[1] O.G. DIBUA,[1] and M.A. CULLINAN[1,2]

1.—Department of Mechanical Engineering, The University of Texas at Austin, 204 E. Dean Keeton Street, Stop C2200, ETC 4.154, Austin, TX 78712-1591, USA. 2.—e-mail: Michael.Cullinan@austin.utexas.edu

Copper nanoparticles (NPs), due to their high electrical conductivity, low cost, and easy availability, provide an excellent alternative to other metal NPs such as gold, silver, and aluminum in applications ranging from direct printing of conductive patterns on metal and flexible substrates for printed electronics applications to making three-dimensional freeform structures for interconnect fabrication for chip-packaging applications. Lack of research on identification of optimum sintering parameters such as fluence/irradiance requirements for sintering of Cu NPs serves as the primary motivation for this study. This article focuses on the identification of a good sintering irradiance window for Cu NPs on an aluminum substrate using a continuous wave (CW) laser. The study also includes the comparison of CW laser sintering irradiance windows obtained with substrates at different initial temperatures. The irradiance requirements for sintering of Cu NPs with the substrate at 150–200°C were found to be 5–17 times smaller than the irradiance requirements for sintering with the substrate at room temperature. These findings were also compared against the results obtained with a nanosecond (ns) laser and a femtosecond (fs) laser.

INTRODUCTION

Recently, the sintering of nanoparticles (NPs) has attracted much interest as an alternative to conventional integrated circuit (IC) fabrication techniques.[1–5] The ever-increasing demand for packing more input–output (I/O) pin counts within a small area to improve the performance and functionality of IC devices is fueling this growth in interest in sintering of NPs.[6,7] Presently, interconnection traces are designed to be on the order of 15–25 μm in width and 20 μm in thickness.[8] To increase the I/O packing density, it is desired to be able to produce structures with much smaller dimensions and pitch. A new additive manufacturing technique called the micro-scale selective laser sintering system (μ-SLS) has been developed to produce micron-sized features on a variety of substrates.[2,8,9] The system uses Cu NP inks as the primary material to fabricate 1-μm-sized features.

A number of research studies have been carried out on studying the sintering of silver (Ag) and gold (Au) nanoparticles because of the stability of these materials.[4,5,10] However, there has been limited research studying the sintering of Cu NPs until recently.[11–13] The authors have presented recent studies on the sintering characteristics of Cu NPs using pulsed lasers and have also reported on the impact of substrate diffusivity on the fluence/irradiance requirements for sintering of Cu NPs.[1,14,15] In this study, the authors present their experimental findings on the sintering irradiance requirements using a continuous wave (CW) laser and compare them with the results from pulsed laser experiments. The study presented also includes a comprehensive investigation of the effect of the substrate's initial temperature on the sintering irradiance requirements. The experiments were conducted with two different thicknesses of Cu layers—0.4 μm and 1.2 μm on an aluminum substrate with four different exposure times, 10 ms, 50 ms, 200 ms, and 500 ms. Sintering irradiance data from these experiments were compiled and classified into different regions including no sintering, weak sintering, good sintering and melting on the processing window.

(Published online November 27, 2017)

EXPERIMENTAL SETUP

A Cu NP ink (CI005-G from Intrinsiq Materials Inc.) with an average particle size of 100 nm was employed in this study. Two different thicknesses of Cu NP films, 0.4 ± 0.2 μm and 1.2 ± 0.2 μm, were prepared by spin coating the NP dispersed ink on the aluminum substrate using an EZ 6 Spin coater (Best Tools, LLC). The films were then heated at 85°C for 15 min on a hot plate.

A 3 W diode pumped solid state (DPSS) laser (Lasever Inc.) with a central wavelength of 532 nm was used as the laser source. The laser beam was Gaussian (waist diameter, 3 mm) and was focused through a 50X (NA–0.55) long working distance objective onto the samples through a series of mirrors and mechanical shutter (see supplementary Figure S1 for experimental setup). The laser powers were measured using a thermal power measurement sensor (Ophir optronics, 10A-P P/N 7Z02649). Additionally, a CCD camera was installed for focusing the beam and spot size determination. A ceramic plate heater held to the XY stage using a clamp was used to heat the samples to three different temperatures: 100 ± 10°C, 150 ± 10°C, and 200 ± 10°C. Temperature measurements were obtained using a K-type thermocouple.

SINTERING RESULTS

The laser powers for these experiments were varied from 40 ± 5 mW to 1000 ± 30 mW, and the spot size was fixed at 16 ± 4 μm. This corresponds to an irradiance range from 19,894 ± 10,253 W/cm^2 to 497,359 ± 249,127 W/cm^2 [see supplementary information (b) for irradiance calculation and supplementary Table S1 for list of irradiances].

Four different exposure times (10 ms, 50 ms, 200 ms, and 500 ms) were used to investigate the effects of changing exposure time on the sintering irradiance requirement. The spots were classified into four categories depending upon the morphology of the sintered spot obtained.[1] The categories were (1) no sintering: spots not affected by the laser, i.e., no necking between particles was observed; (2) weak sintering: spots that showed considerable necking between the particles but the necking was not uniform across the spot area; (3) good sintering:

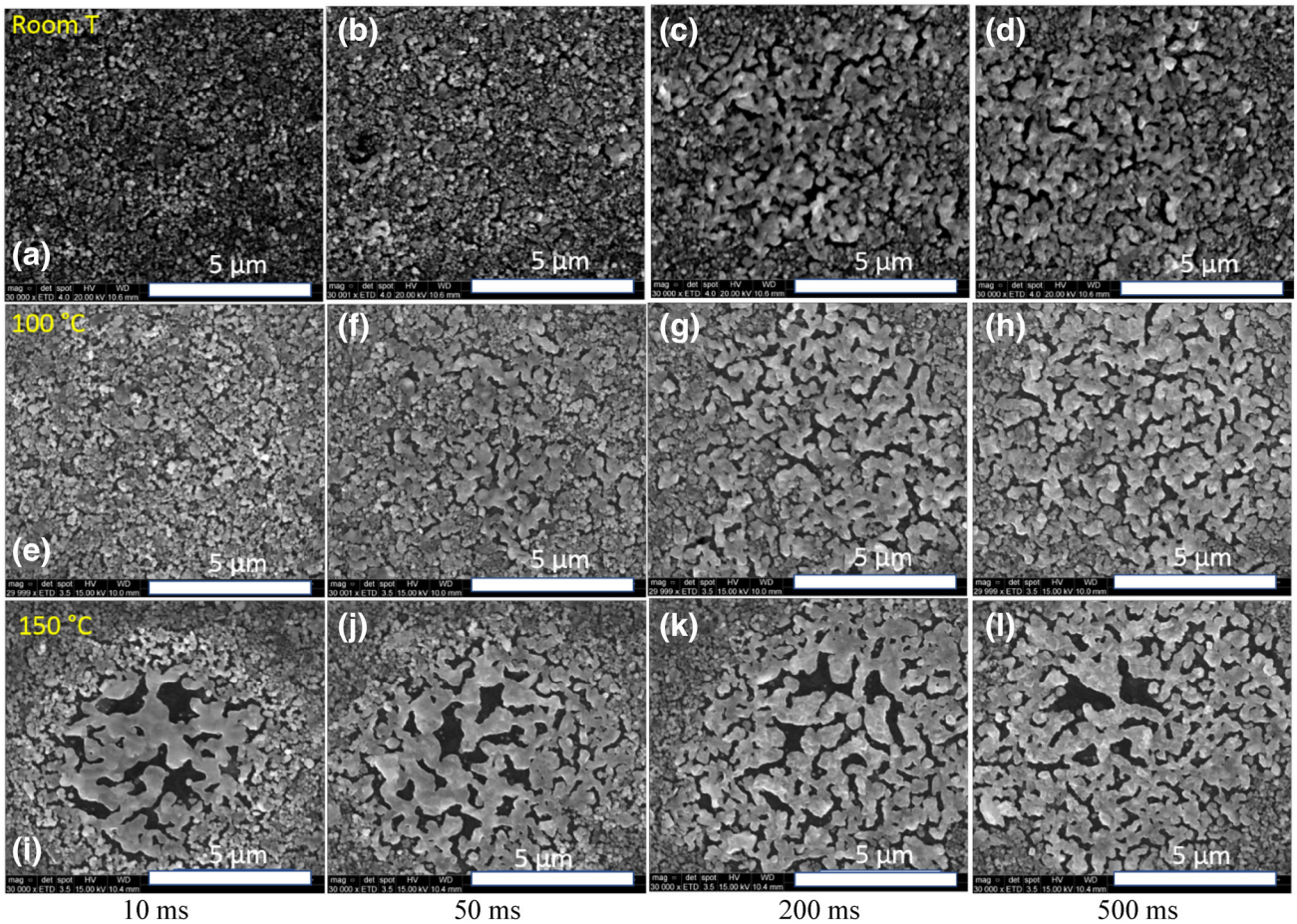

Fig. 1. SEM images of spots sintered on a 0.4 μm thick Cu layer with a power density of 99.47 ± 49.98 kw/cm^2 for (a) 10 ms (b) 50 ms (c) 200 ms and (d) 500 ms with substrate at room temperature; (e) 10 ms (f) 50 ms (g) 200 ms and (h) 500 ms with substrate at 100°C; (i) 10 ms (j) 50 ms (k) 200 ms (l) 500 ms with substrate at 150°C.

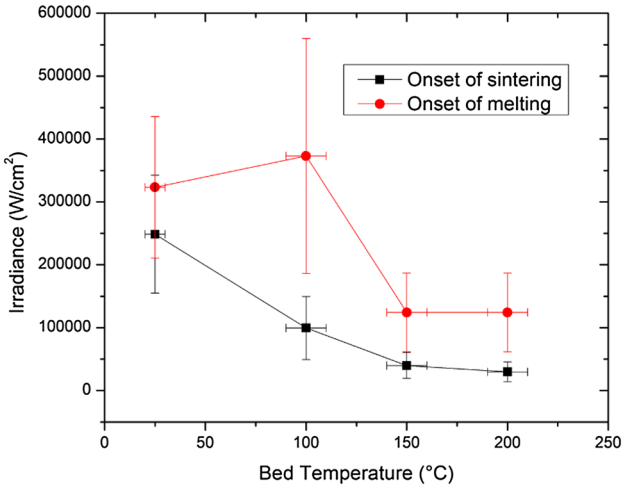

Fig. 2. Variation in onset of sintering and melting irradiances with bed temperature with an exposure duration of 200 ms on a 1.2 μm thick Cu layer.

spots that showed significant necking between all the particles in the spot area; (4) melting/damage: spots that showed formation of liquid melt pools and the hydrodynamics of melt pool forced it to flow to the periphery of the spot. In addition to these thresholds, the sintering window was defined as the range of irradiances between onset of sintering and onset of melting irradiances. Figure 1 shows the SEM images of sintered spots on a 0.4-μm-thick Cu layer with different substrate temperatures and exposure times with an incident irradiance of 99.47 ± 49.98 kW/cm^2. SEM images in each row show the spots sintered at a constant substrate temperature, while those in each column show spots sintered at the same exposure duration.

In well-sintered spots, such as Fig. 1g and h (see supplementary Figure S2 for higher magnification images), the particles were all connected to one another through a series of inter-particle

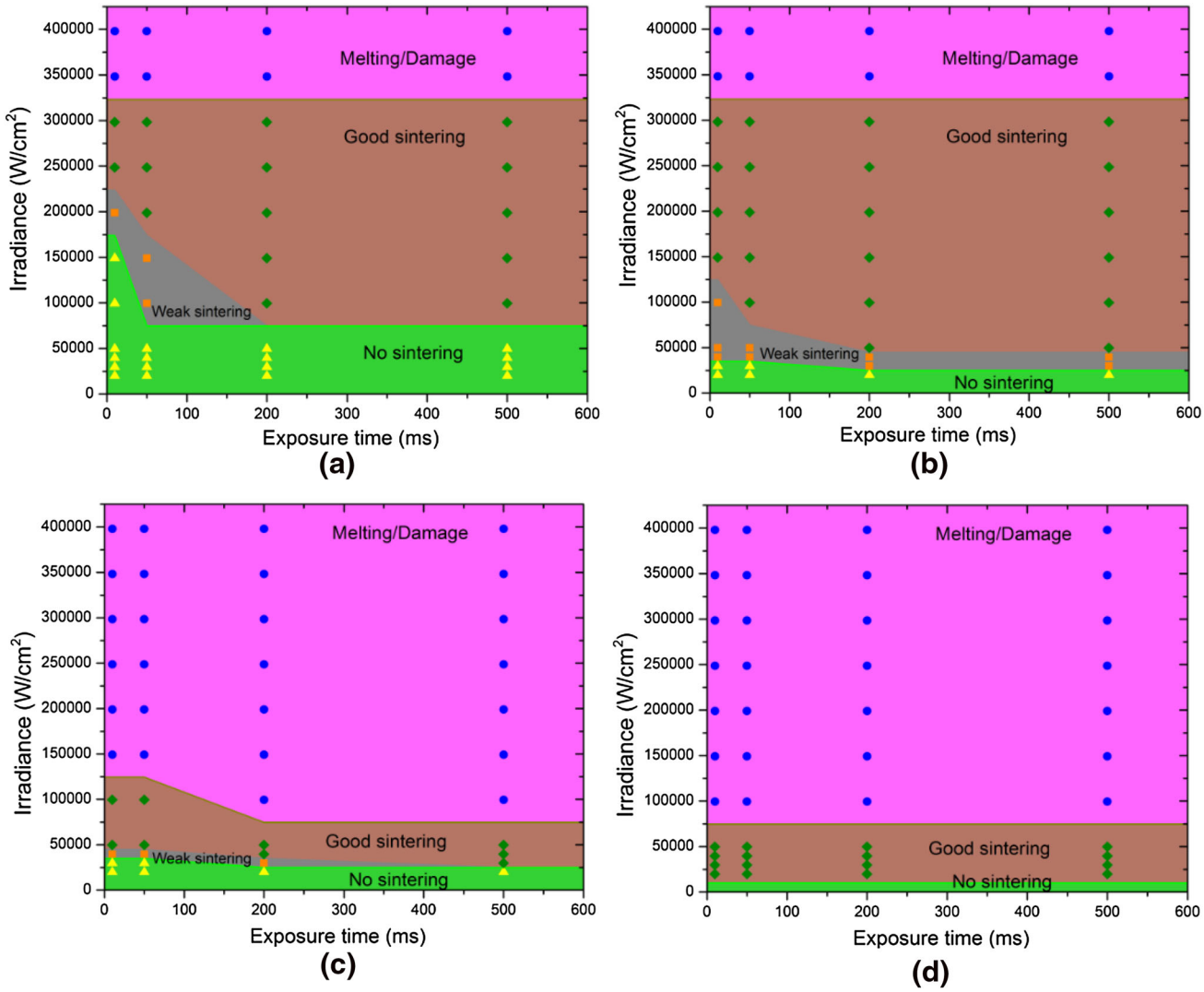

Fig. 3. Processing window for different sintering regions for 0.4 μm thick Cu sample on Al substrate at (a) room temperature (b) 100°C (c) 150°C (d) 200°C.

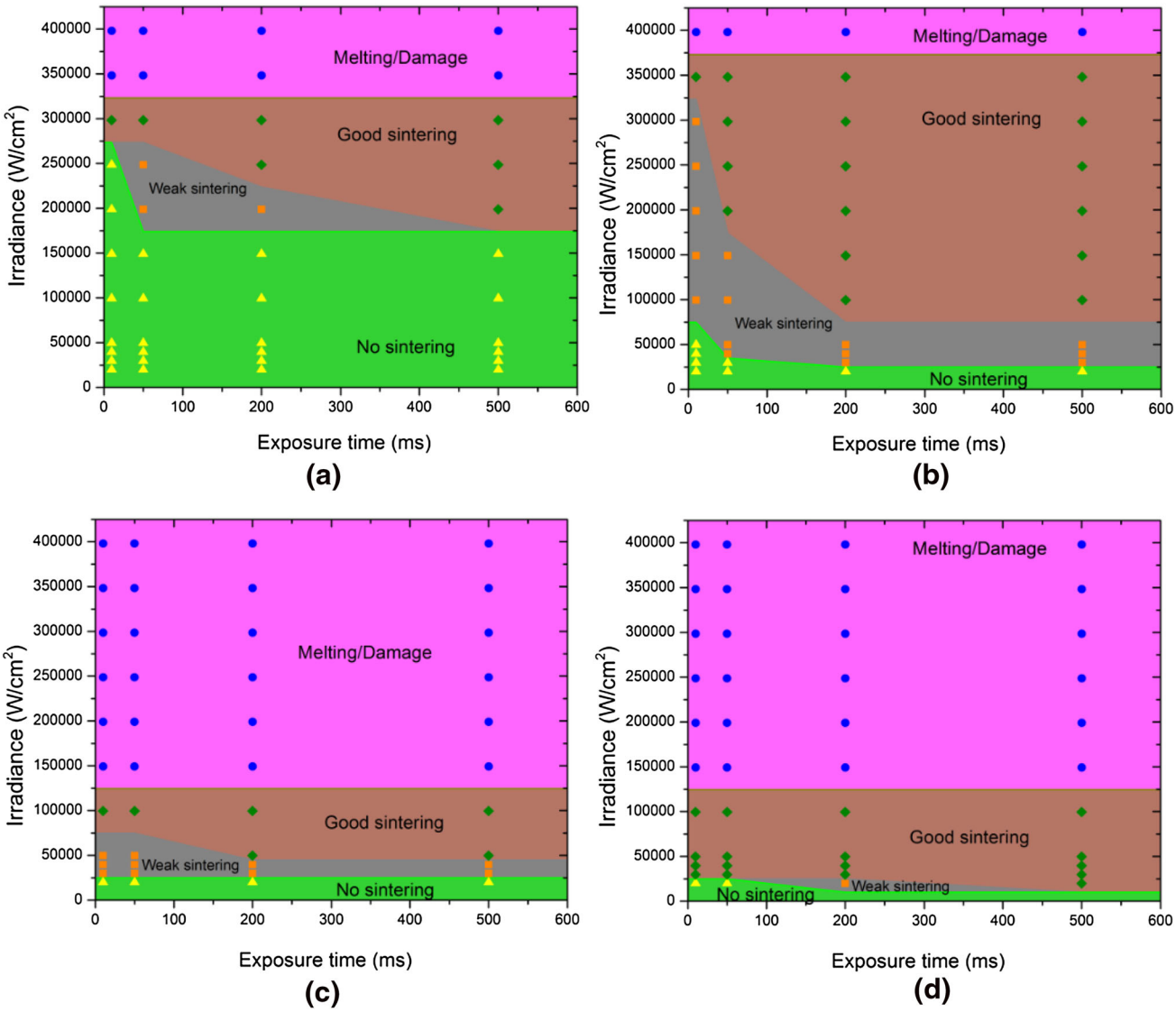

Fig. 4. Processing window for different sintering regions for 1.2 μm thick Cu sample on Al substrate at (a) room temperature (b) 100°C (c) 150°C (d) 200°C.

connections. This continuity of the particles in the spot area is essential to ensure that the sintered spots match the physical, thermal and electrical properties of the bulk material as closely as possible.

DISCUSSION

From the SEM images shown in Fig. 1 (see supplementary Figure S3 for SEM images of spots sintered on the 1.2-μm-thick Cu layer), it is evident that sintering in the spot area is enhanced with increasing bed temperature at the same irradiance level and same exposure duration. This can also be interpreted as the reduction in irradiance requirement for onset of sintering with increasing bed temperatures. The plot in Fig. 2 shows the trend of onset of sintering irradiance with bed temperature (at a constant exposure duration of 200 ms on a 1.2-μm-thick Cu layer) and corroborates this trend of decreasing irradiance requirement with increasing bed temperatures.

In addition to the onset of the sintering threshold, the melting threshold goes down with increasing bed temperatures for both thicknesses of Cu NP layers, as seen from the processing windows shown in Figs. 3 and 4. This reduction in the sintering and melting thresholds can be explained by the fact that as the bed temperature is increased, lower energy is required by NPs to reach the onset of sintering temperature[2] or melting temperature. Also, since the temperature difference to be overcome is

Table I. Average sintering and melting/damage irradiance range using different types of laser and at different bed temperatures for 1.2 μm thick Cu layer

			CW Laser			
	FS laser[1]	NS laser[1]	Room T	100°C	150°C	200°C
Average onset of sintering irradiance (W/cm^2)	55 ± 13	318 ± 90	174,075 ± 87,617	74,603 ± 37,672	34,814 ± 18,117	9947 ± 5126
Average onset of melting/damage irradiance (W/cm^2)	220 ± 42	1655 ± 350	323,283 ± 112,347	373,019 ± 186,931	124,340 ± 62,624	124,340 ± 62,624

smaller, the particles reach the sintering temperature in a smaller time duration, reducing the heat transfer losses in the system. Thus, raising the bed temperature close to the onset of sintering temperature provides two-way benefits with respect to the sintering irradiance requirement.

Figure 1 also shows the variation in sintering extent/quality with exposure duration at different substrate temperatures. The extent of sintering was found to improve with longer exposure times. However, longer exposure times led to spots with bigger heat-affected zones. Processing windows shown in Figs. 3 and 4 indicate an inverse relationship between the irradiance thresholds for sintering and melting windows and exposure duration. This is in contrast to the variation of these thresholds using pulsed laser sintering with exposure duration.[1,15] Since pulsed lasers (ns, ps, and fs) have much longer periods between two pulses compared to the pulse duration (with a repetition rate $<$ 100 kHz, the time between pulses $>$ 10 μs), the NPs return to the room temperature within that time duration, resulting in minimal influence of past train of pulses on the sintering characteristics. Thus, sintering and melting thresholds using pulsed lasers tend to be independent of exposure duration. Using CW lasers, there is a continuous supply of laser energy to the particles and there is no time window for NPs to return to the room temperature. Due to this accumulation of the laser energy over time, the thresholds vary with exposure times. These thresholds were also found to be higher for the 1.2-μm samples at all substrate temperatures compared to 0.4-μm samples.

The sintering window using a CW laser with substrate at different temperatures was compared with average irradiance requirements using pulsed (ns and fs) lasers from recent studies conducted on sintering characteristics of Cu NPs.[1,15] With substrate at room temperature, the sintering irradiance window using a CW laser was found to be significantly higher than the irradiance window using pulsed lasers for both thicknesses (see process windows in Figs. 3 and 4). Table I lists the onset of sintering and onset of melting irradiances for 1.2-μm-thick Cu layer using different lasers and bed temperatures. Peak powers developed during sintering of NPs using pulsed lasers are orders of magnitude higher than the powers developed during CW laser sintering, and this is the reason for higher irradiance requirements for CW laser sintering. It was also interesting to note that the sintering irradiance window reduced significantly with increasing bed temperature. The onset of sintering irradiance was reduced by a factor of 17.5 ± 12.6 with a bed temperature at 200°C, and it was reduced by a factor of 5.0 ± 3.6 with bed temperature at 150°C. Another advantage of performing laser sintering with elevated bed temperature is the smaller residual thermal stress in the finished part compared to sintering with the bed at

room temperature.[16,17] However, it is important to consider the effects of oxidation of NPs at elevated bed temperatures. In general, at elevated bed temperatures, NPs tend to oxidize much faster compared to oxidation at room temperature,[18,19] leading to a higher sintering temperature, which in turn increases the sintering irradiance requirement. However, the NP ink used in this study comprises NPs with a protective coating of polyvinylpyrrolidone (PVP), which prevents the particles from oxidation and agglomeration. PVP has been found to decompose at temperatures as high as 450°C;[20] thus, heating the bed to 200°C does not oxidize the particles, which ultimately results in a lower energy requirement for sintering.

CONCLUSION

In this study, we presented a comprehensive investigation of the dependence of sintering irradiance using a CW laser with substrate initial temperatures. The substrates were heated to three different temperatures, 100°C, 150°C, and 200°C, and the experiments were conducted to identify the irradiance range for (1) no sintering, (2) weak sintering, (3) good sintering and (4) melting on the processing window. These ranges were then compared with the results obtained using CW laser sintering at room temperature. In addition to this, the sintering irradiance window from these experiments was also compared with the average sintering irradiances using ns and fs lasers. The variation of these ranges with exposure duration was also identified. The sintering irradiance threshold was reduced by a factor of 5 ± 3.6 with substrate at 150°C and by a factor of 17.5 ± 12.6 with substrate at 200°C when compared to the irradiance threshold with substrate at room temperature. This directly affects the maximum power requirement of the laser and can substantially reduce the cost of systems employing the CW laser as the laser source for sintering in additive manufacturing of electronic structures. With the knowledge of irradiance requirements for sintering, future work will include sintering experiments with the optical sub-system of μ-SLS at different bed temperatures.

ACKNOWLEDGEMENTS

The authors would like to acknowledge the financial support received from NXP Semiconductors. The authors would like to thank Mr. Chee Seng Foong of NXP Semiconductors for his valuable inputs to the discussion on the sintering experiments.

ELECTRONIC SUPPLEMENTARY MATERIAL

The online version of this article (https://doi.org/10.1007/s11837-017-2668-0) contains supplementary material, which is available to authorized users.

REFERENCES

1. N.K. Roy, O.G. Dibua, W. Jou, F. He, J. Jeong, Y. Wang, and M.A. Cullinan, *J. Micro Nano Manuf.* https://doi.org/10.1115/1.4038455.
2. N. Roy, A. Yuksel, and M. Cullinan, in *ASME International Manufacturing Science and Engineering Conference, Proceedings*, vol. 3, p. V003T08A002 (2016).
3. N.K. Roy, A. Yuksel, and M.A. Cullinan, in *26th Solid Freeform Fabrication Symposium Proceedings*, vol. 772 (2015).
4. I. Theodorakos, F. Zacharatos, R. Geremia, D. Karnakis, and I. Zergioti, *Appl. Surf. Sci.* 336, 157 (2015).
5. K. An, S. Hong, S. Han, H. Lee, J. Yeo, and S.H. Ko, *ACS Appl. Mater. Interfaces* 6, 2786 (2014).
6. A. Allan, D. Edenfeld, W.H. Joyner, A.B. Kahng, M. Rodgers, and Y. Zorian, *Computer* 35, 42 (2002).
7. C. Barrett, in *Symposium on VLSI Technology, Digital Technical Paper*, vol. 15, p. 7 (1993).
8. N.K. Roy, C.S. Foong, and M.A. Cullinan, in *27th Solid Freeform Fabrication Symposium Proceedings*, vol. 1495 (2016).
9. N.K. Roy and M.A. Cullinan, in *26th Solid Freeform Fabrication Symposium Proceedings*, vol. 134 (2015).
10. Y. Son, T.W. Lim, J. Yeo, S.H. Ko, and D.-Y. Yang, in *10th IEEE International Conference on Nanotechnology*, vol. 7, p. 390 (2010).
11. M. Zenou, O. Ermak, A. Saar, and Z. Kotler, *J. Phys. D Appl. Phys.* 47, 025501 (2014).
12. M.D. Shirk and P.A. Molian, *J. Laser Appl.* 10, 18 (1998).
13. E.G. Gamaly, A.V. Rode, B. Luther-Davies, and V.T. Tikhonchuk, *Plasma Phys.* 9, 949 (2001).
14. N.K. Roy, W. Jou, H. Feng, J. Jeong, Y. Wang, and M.A. Cullinan, in *ASME International Manufacturing Science and Engineering Conference, Proceedings* (in press).
15. N. Roy, O. Dibua, C.S. Foong, and M.A. Cullinan, in *Proceedings of the ASME 2017 International Technical Conference and Exhibition on Packaging and Integration of Electronic and Photonic Microsystems InterPACK2017* (in press).
16. I. Gibson and D. Shi, *Rapid Prototyp. J.* 3, 129 (1997).
17. S. Kumar, *JOM* 55, 43 (2003).
18. S. Samal, *High Temperature Corrosion*, ed. Z. Ahmad (Rijeka: InTech, 2016), p. 101.
19. A. Auge, A. Weddemann, B. Vogel, F. Wittbracht, and A. Hütten, in *Proceedings of the COMSOL Conference, Milan* (2009).
20. Y.K. Du, P. Yang, Z.G. Mou, N.P. Hua, and L. Jiang, *J. Appl. Polym. Sci.* 99, 23 (2006).